



SELF-SUSTAINED OSCILLATIONS IN FLOWS AROUND LONG BLUNT PLATES

K. HOURIGAN, M. C. THOMPSON AND B. T. TAN

*Fluids Laboratory for Aeronautical and Industrial Research (FLAIR)
Department of Mechanical Engineering, Monash University
Clayton, 3800, Australia*

(Received 10 September 2000, and in final form 10 November 2000)

The presence of flow separation from both leading and trailing edges of elongated bluff bodies leads to vortex interactions and resonances not observed in shorter bodies such as circular and square cylinders. Stepwise behaviour in the Strouhal number with increasing plate chord-to-thickness ratio has been observed for long bodies in a number of different situations: natural shedding, under transverse forcing, and with excited duct modes. In the present study, an investigation is made of the predicted unforced laminar flow around long plates (up to chord, c , to thickness, t , ratio $c/t = 16$). The two main types of plate geometry considered are rectangular plates and plates with an aerodynamic leading edge. The rectangular plate represents a geometrical extension of the normal flat and square plates. The aerodynamic leading-edge plate is a natural precursor to the rectangular plate because the vortex shedding is only from the trailing edge. The natural flow around rectangular plates is of greater complexity due to the interaction between the leading- and trailing-edge shedding. The previously neglected influence of the trailing-edge vortex shedding is found to play an important role in the stepwise progression of the Strouhal number with chord-to-thickness ratio. In addition, the formation of three-dimensional patterns in the boundary layer along the plate and in the trailing-edge wake is predicted. The predicted boundary layer hairpin vortices are compared with previous observations and the predicted streamwise modes in the wake are compared with those found in the case of circular cylinders.

© 2001 Academic Press

1. INTRODUCTION

THE FLOW around elongated bluff bodies, even of simple geometries such as rectangular plates, can result in a number of different local instabilities. Moreover, the complexity of the flow is increased as a result of interaction between upstream and downstream flow structures and the interaction of flow and solid structures. These interactions can lead to global instabilities arising in the flow. In this paper, we explore some of the different two- and three-dimensional instabilities that occur in flow around two-dimensional blunt plates at relatively low Reynolds number.

Instability in the wake is present in most bluff bodies above a critical Reynolds number. With long bluff bodies, it is possible for the flow to separate at the leading edge and reattach while shedding large-scale vortices. A detailed investigation into the nature of this separated and reattaching flow is found in Cherry *et al.* (1984). Two instabilities are involved: the Kelvin–Helmholtz instability present in the shear layer; and the instability causing the large-scale shedding. In combination, there is a weak flapping of the shear layer and an irregularity of shedding. Experiments by Soria *et al.* (1993) used long rectangular plates to isolate any trailing edge effects. The separating and reattaching flow was shown to be

predominantly convectively unstable and receptive to a broad range of frequencies. The weak flapping of the shear layer without external perturbation could be the result of regions of local absolute instabilities.

Another type of global instability occurs when a local convective instability interacts with a solid boundary downstream. Disturbances from the object downstream propagate upstream to complete a feedback loop. For a rectangular plate, this phenomenon is observed when the shear layer from the leading edge is influenced by the trailing edge. This type of instability is similar to when jet or mixing layers impinge on some downstream geometry, for example a bluff body, wall or sharp edge. A comprehensive review is found in Rockwell & Naudascher (1979). The concept of global instability was associated with these sorts of flows by Rockwell (1990).

The flow around rectangular plates in the absence of any external forcing has been studied previously both experimentally and numerically (Nakamura *et al.* 1991; Ohya *et al.* 1992). The vortex shedding from the leading edge of the plate generally locked to a single frequency at low Reynolds numbers [up to $Re \sim 3000$, Nakamura *et al.* (1991)]. This instability was thought to rely on the interaction of the leading-edge vortices with the trailing edge to generate a pressure pulse. This pulse locks the leading-edge shedding and completes the feedback loop. The pressure pulse is relatively weak and therefore this locked response is restricted to low Reynolds numbers and only a limited range of chord-to-thickness ratios. It was initially classified as an impinging shear layer (ISL) instability by Nakamura & Nakashima (1986) and Nakamura *et al.* (1991) because in some cases (where the chord-to-thickness ratios were low), the shear layer directly interacted with the trailing edge; this has similarities with the instability in cavity flows. Later studies (Naudascher & Wang 1993; Hourigan *et al.* 1993; Naudascher & Rockwell 1994; Mills *et al.* 1995; Mills 1998; Tan *et al.* 1998) preferred the description impinging leading-edge vortex (ILEV) instability because it better describes the process wherein leading-edge vortices are shed, convected downstream and then interact with the trailing edge. A result of this instability is the occurrence of distinct integer shedding modes (denoted by n , the number of pairs of vortices distributed along the plate at any time). Observationally, as the plate chord-to-thickness ratio is increased, the Strouhal number of vortex shedding based on chord (St_c) shows a stepwise response with each subsequent step corresponding to a higher shedding mode.

In the studies undertaken previously on the natural shedding modes for elongated plates, the presence of trailing-edge vortex shedding was generally not observed or included in discussions. In the case of Ohya *et al.* (1992) where it was observed, the trailing-edge shedding was not considered to be part of the feedback loop but merely led to contamination of the downstream wake. The present study approaches the problem of natural shedding modes from a different perspective in order to establish the importance of trailing-edge shedding to the self-sustained oscillations. As a starting point, the case of a blunt plate with an aerodynamic leading edge is investigated numerically to understand the trailing-edge shedding in the absence of upstream vortex interference. Then, the two-dimensional flow around rectangular plates is studied with a view to understanding the role of the leading-edge vortices in interfering with the trailing-edge shedding and the occurrence of frequency stepping. Finally, some predictions are undertaken to confirm the continued presence of trailing-edge vortex shedding and the locking of the vortex shedding when extended to three dimensions. In addition, the formation of three-dimensional patterns in the boundary layer along the plate, and in the trailing-edge wake, are investigated. The boundary layer hairpin vortical structures are compared with those from the experiments of Sasaki & Kiya (1991) and the predicted streamwise modes in the wake are compared with those found in the case of circular cylinders (Williamson 1988; Thompson *et al.* 1996; Barkley & Henderson 1996).

2. NUMERICAL METHOD

The wake of a fixed circular cylinder has been well characterised over the transition region (Reynolds number ranging from 180 to 300). Following the pioneering numerical work of Karniadakis & Triantafyllou (1992), Thompson *et al.* (1994, 1996) first predicted the wavelengths of both wake Modes, A and B, and validated those against the rigorous measurements of Williamson (1988). The spectral-element method used in that study was employed in the current study. The spectral-element method is a high-order finite-element approach. Within each element, the nodes correspond to Gauss–Lobatto points and Gauss–Legendre–Lobatto quadrature is used to approximate the integrations over elements resulting from the application of the Galerkin finite-element method to the Navier–Stokes equations. For high-order elements, this approach is far more economical than equispaced nodes, while still maintaining the spectral convergence rate.

The time-stepping method used was a classical three-step approach described by Karniadakis *et al.* (1991). In the spanwise direction for the three-dimensional predictions, a Fourier expansion was used, resulting in the equations decoupling for each Fourier mode.

The conditions applied at the boundaries of the computational domain were: (i) no slip on the plate; (ii) zero normal velocity derivative at the outflow boundary; and (iii) on the side and inflow boundary, the velocity was taken as uniform in the horizontal direction. A typical computational mesh displaying the macro-elements employed for the elliptical leading-edge plate is shown in Figure 1.

Before the detailed investigation into the flow around long plates was undertaken, some preliminary simulations were performed to determine an adequate domain size and resolution. For flow around bluff bodies, the predictions of surface pressure can be significantly altered if the boundaries are too close to the body (Barkley & Henderson 1996). The two-dimensional simulations were intended to produce quantitative predictions of base pressure and forces on the plate and therefore some preliminary simulations were performed to determine an adequate domain size. The resolution was confirmed to be adequate (to within 2%) by performing simulations with higher spatial and temporal resolution.

3. RESULTS AND DISCUSSION

Figure 2 shows schematics of the long plates studied together with their associated flow features. The flow around plates with only trailing-edge vortex shedding was investigated as a precursor to the study of flows around rectangular plates.

3.1. FLOW AROUND ELLIPTICAL LEADING-EDGE PLATES

The shedding frequency predicted by the simulation was compared with the results obtained experimentally by Eisenlohr & Eckelmann (1988). Simulations were performed for a plate with $c/t = 7.5$ between $Re = 200$ and 700 ; the leading edge was semi-elliptical with a 5:1 axes ratio. The shedding frequency was extracted from the base pressure trace, which in all these cases asymptoted to a periodic state.

Eisenlohr & Eckelmann (1988) found a correlation between the reduced shedding frequency (F_r) and the Reynolds number (Re_r) if the characteristic length was taken as the plate thickness plus twice the displacement thickness at the trailing edge. The simulations were in good agreement with these results (see Figure 3). The plots show that the rate of increase of F_r with Re_r is visually indistinguishable between the predictions and experiments. The predicted F_r at all but the lowest Reynolds number simulated were within the range of experimental uncertainty. This demonstrated that the simulation was able to

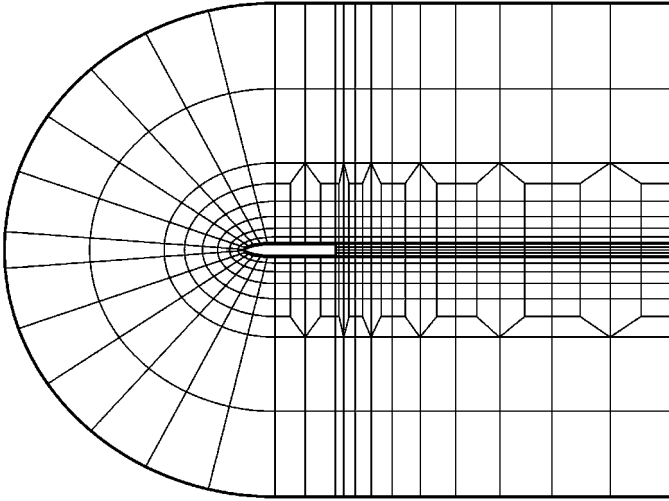


Figure 1. The computational mesh showing the macro-elements for an elliptical leading-edge plate with $c/t = 7.5$.

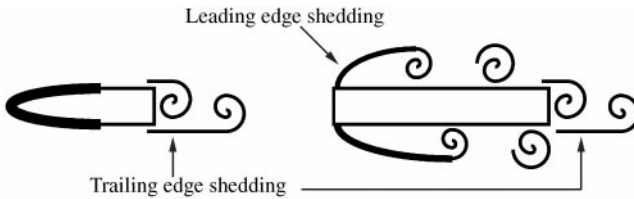


Figure 2. A sketch of the vortical flow structures for flow past an elliptical leading-edge plate and a rectangular plate.

capture most of the experimental trends; differences may have been due to the much longer plates and higher Reynolds numbers (resulting in three dimensionality) used in the experiments.

3.2. LEADING- AND TRAILING-EDGE SHEDDING: RECTANGULAR PLATES

3.2.1. Simulation results

Several simulations were performed to study the effect of Reynolds number. Flow around plates with chord-to-thickness ratios of $c/t = 3$ and 10 were simulated at $Re = 300, 400$ and 500. All simulations with $c/t = 3$ locked to the first shedding mode ($n = 1$) while at $c/t = 10$, the flow locked to the third shedding mode ($n = 3$) when $Re = 300$ and 400. At $Re = 400$, there were small fluctuations between periods in the base pressure trace and at $Re = 500$, the flow no longer locked to a particular shedding mode; there were several frequencies present in the base pressure trace. When the flow was locked to a particular mode, varying the Reynolds number had only a small influence on the shedding frequency (i.e., less than 10%). Nakamura *et al.* (1991) also found that the shedding frequency was independent of Reynolds number when this mechanism locked the flow. The base pressure trace showed that the mean and standard deviation increased with Reynolds number for all cases where

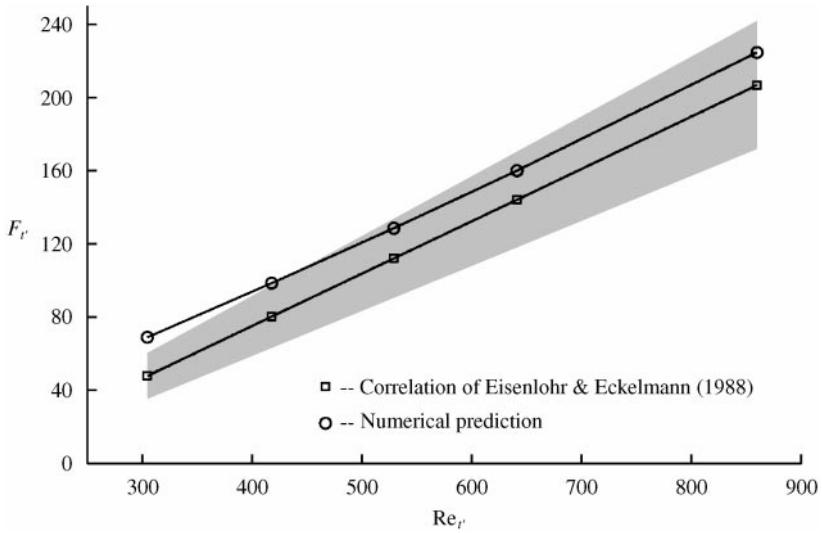


Figure 3. A plot of the nondimensional shedding frequency, F_v , as a function of the Reynolds number Re_v for the flow around an elliptical leading-edge plate with $c/t = 7.5$. The correlation obtained from experiments by Eisenlohr & Eckelmann (1988) is plotted for comparison. The shaded region is indicative of the spread in the experimental data.

the flow was locked. There was a drop in the mean and standard deviation when the Reynolds number was increased and the flow no longer locked to a shedding mode.

Next, the chord-to-thickness ratio was systematically varied in unit increments from $c/t = 3$ to 16 at $Re = 400$. The flow locked to a shedding mode for each c/t between 3 and 10 and also at $c/t = 13$. Vorticity plots in Figure 4 show that for $c/t = 3-5$, the vortex shedding locked to $n = 1$; for $c/t = 6-8$, it locked to $n = 2$; for $c/t = 9$ and 10, it locked to $n = 3$; and for $c/t = 13$, it locked to $n = 4$. The Strouhal number based on chord approximately corresponds to $St_c = 0.55n$ for all these cases. The factor 0.55 represents the mean convection velocity, normalized by the free-stream velocity, of the vortices along the plate. The base pressure trace in Figure 5 shows a higher level of fluctuation between periods towards the higher chord-to-thickness ratio end of each shedding mode. The spectrum taken from the base pressure trace when $c/t = 11$ (not locked) was found to contain three frequencies, one corresponding to the $n = 3$ shedding mode, another to a frequency that was in the middle of the $n = 2$ and 3 shedding mode, plus a third corresponding to the nonlinear interaction between these two modes.

The effect of the global instability is also seen in the variation of the base pressure and forces on the plate (see Figure 6). The mean base suction and drag forces are generally higher at the lower c/t end of the step and decrease with c/t . This trend continues even to chord-to-thickness ratios that no longer lock to a single frequency. The standard deviation of lift coefficient varies approximately in inverse proportion to c/t .

Animations of the predicted pressure fields show that the large stepwise changes in the base pressure as the plate chord-to-thickness ratio is increased are due to the return of strong trailing-edge vortex shedding. With increasing chord-to-thickness ratio, the leading-edge vortices are increasingly diffused by the time they reach the trailing edge. When the flow is strongly locked, the leading-edge vortices move almost parallel to the plate into the wake. The dominant fluctuation in pressure at the trailing edge is due to the intense formation and shedding of trailing-edge vortices. An instantaneous plot of the pressure field of the locked flow for $c/t = 10$ is shown in Figure 7. At the trailing edge, more intense

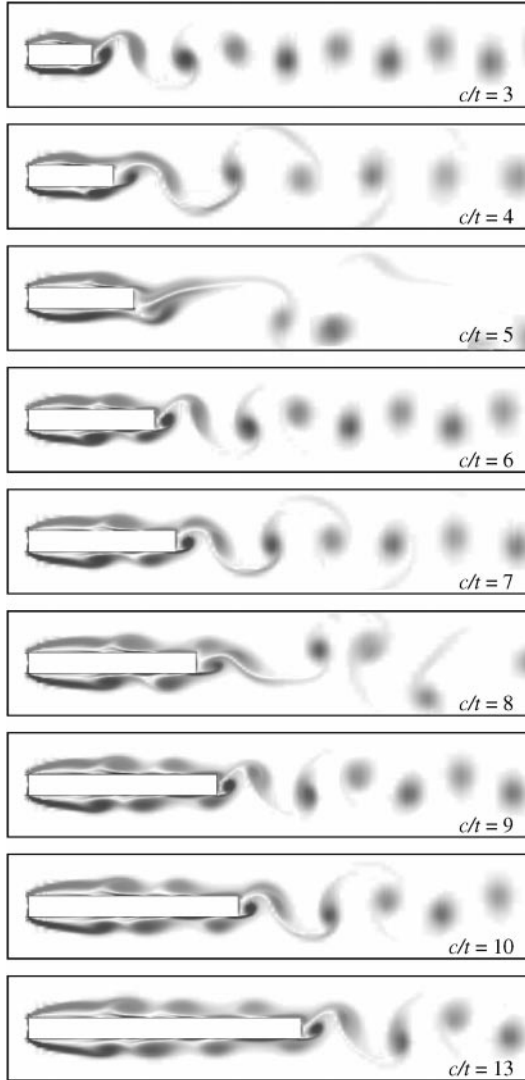


Figure 4. Vorticity plots of flow around rectangular plates at $Re = 400$ taken at approximately the same phase in the shedding cycle for the various chord-to-thickness ratios.

structures are seen to be forming and shedding while the more diffuse leading-edge vortices pass over the top and are merged further downstream. For all the chord-to-thickness ratios, the trailing-edge vortex shedding provided the strong pressure fluctuations at the trailing edge while the leading-edge vortices sometimes acted to frustrate the regularity of this shedding.

3.2.2. On the controlling mechanism

Previous studies and classification associated with the flow around long rectangular plates did not include the important role of shedding from the trailing edge (Nakamura *et al.* 1991; Ozono *et al.* 1992; Naudascher & Wang 1993). In the current simulations, although weak

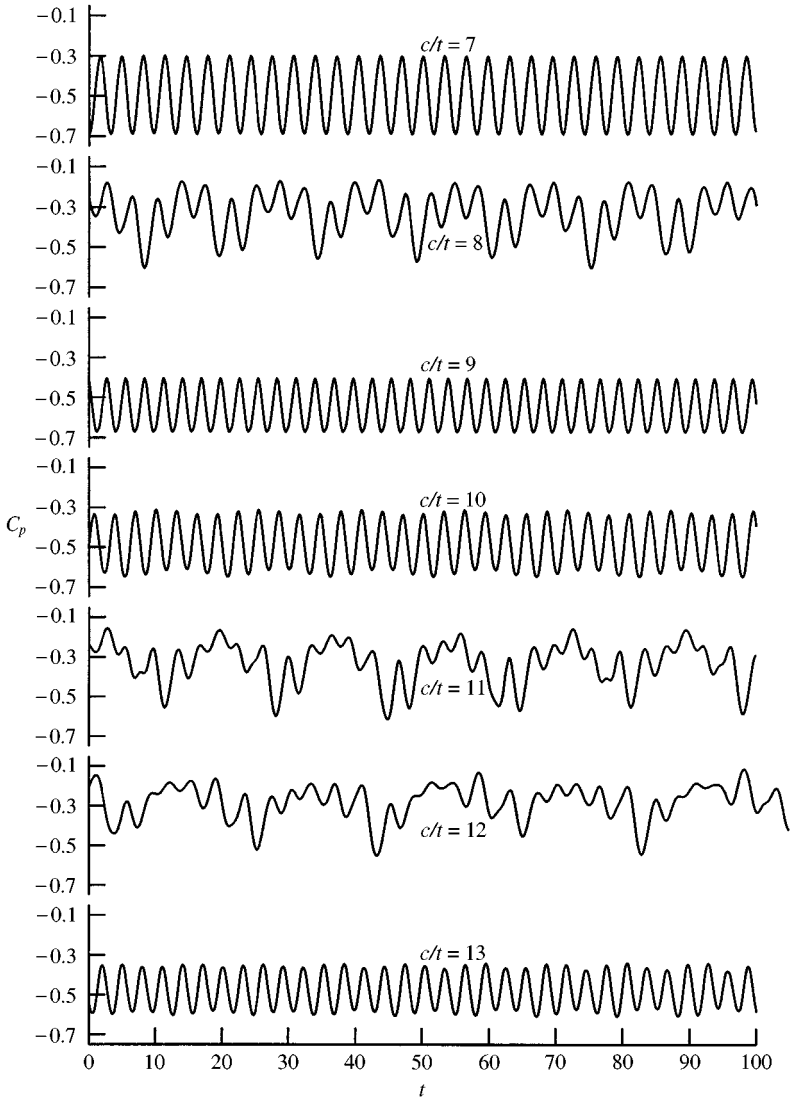


Figure 5. A sample of 100 time units of the base pressure coefficient, C_p , trace for flow around rectangular plates at different chord-to-thickness ratios at $Re = 400$.

pressure fluctuations would occur when the leading-edge vortices pass the trailing edge, strong base shedding is also observed leading to more significant pressure fluctuations. This is seen in the large mean and fluctuating components in base pressure. A description of the different feedback processes for bluff bodies is shown in Figure 8. For short bodies, the leading-edge shear layer can impinge directly on the trailing edge. For longer bodies, vortices are shed from the shear layer at the leading edge. These vortices convect along the plate and interact with the trailing edge. For bodies with streamlined trailing edges [for example, the — section and a wide variety of bluff bodies such as cylinders and square sections fitted with splitter plates (Nakamura 1996)], the leading-edge vortices generate a pressure pulse as they pass the trailing edge. However, for the bodies with bluff trailing edges as in the present case, the leading-edge vortices interact with the shedding at the

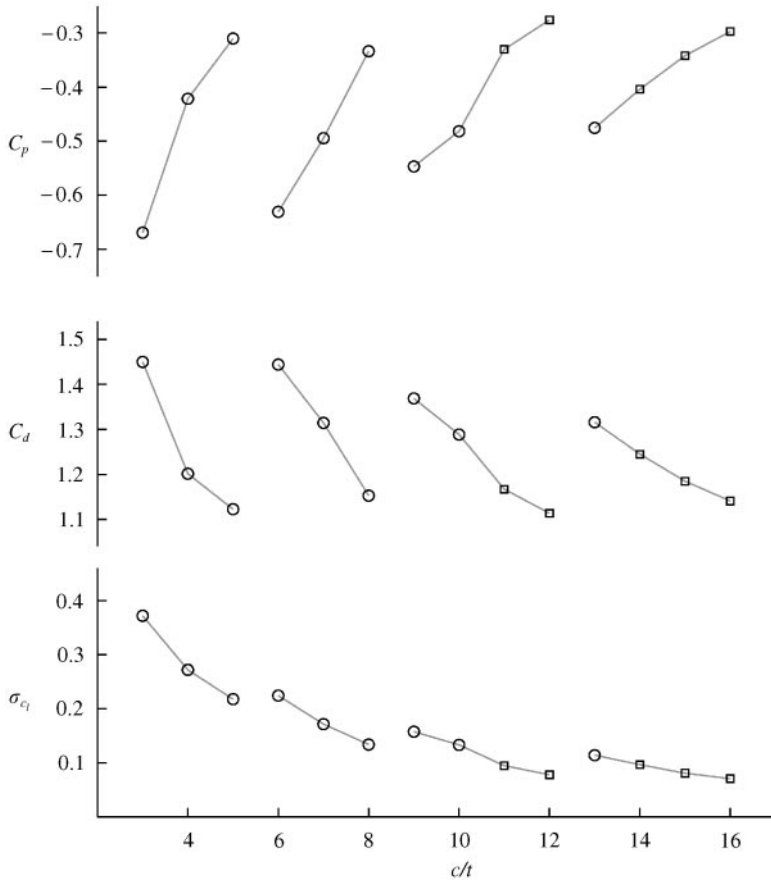


Figure 6. Mean base pressure coefficient, C_p , mean drag coefficient, C_d , and standard deviation of lift coefficient, σ_{C_l} , as a function of the chord-to-thickness ratio for flow around rectangular plates at $Re = 400$. The circular symbols represent cases where the flow shows an association with a particular shedding mode while the squares represent the cases where the flow is not strictly locked to any one shedding mode.

trailing edge. That is, trailing-edge vortices can only form between the passing of leading-edge vortices. Vortices at the trailing edge form from the redeveloped thin boundary layer between vortices, in a manner similar to their formation for the elliptical leading-edge case. The leading-edge vortices punctuate the redeveloped boundary layer and restrict the phases at which trailing-edge shedding can occur. The pressure pulse from the vigorous base shedding then feeds back upstream and controls the leading-edge shedding. The global instability in this case, therefore, consists of a combination of impinging leading-edge vortex shedding (ILEV) and trailing-edge vortex shedding (TEVS).

3.3. THREE-DIMENSIONAL SIMULATIONS

A limited number of three-dimensional flow simulations were performed to study the transitional states for flow around elliptical leading-edge and rectangular plates. The Reynolds numbers in these simulations were chosen to be slightly in excess of the values at which transition from two- to three-dimensional flow occurs. In the aerodynamic leading-edge plate case, the transition in the wake was examined. The spanwise instability of leading-edge vortices was the focus in simulations involving rectangular plates. The nature

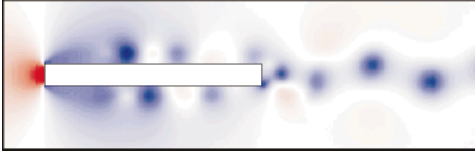


Figure 7. Instantaneous pressure field for a plate with $c/t = 10$. Blue indicates lower pressure, generally indicative of vortex structures, and red higher pressure.

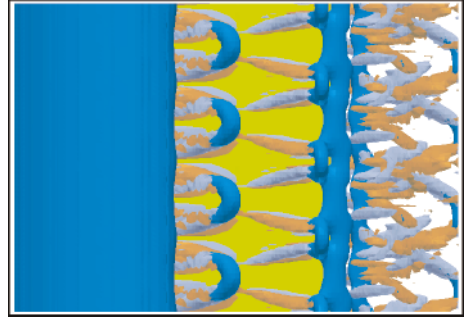


Figure 10. Isosurface plot for predicted flow (left to right) around a rectangular plate with $c/t = 13$ at $Re = 350$ viewed from the top. The normalized value of the isosurface of kinematic pressure is at -0.15 and the values of the streamwise vorticity are at ± 0.8 . Note that the simulated spanwise domain has been doubled for this visualization (and also for Figure 9).

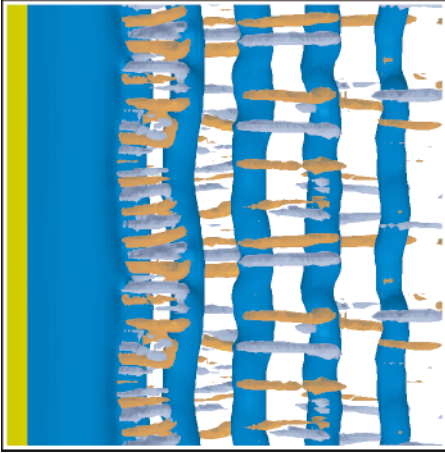
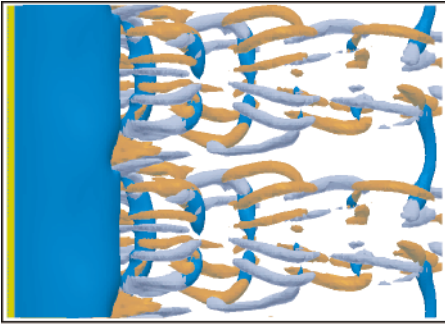


Figure 9. Isosurface plots for predicted flow (left to right) past an elliptical leading-edge plate with $c/t = 2.5$ for $Re = 300$ (top) and $Re = 380$ (bottom). The nondimensionalized values of the kinematic pressure (blue) are -0.25 (top) and -0.20 (bottom), and the streamwise vorticity (red and gray) ± 1.0 (top) and ± 1.2 (bottom).

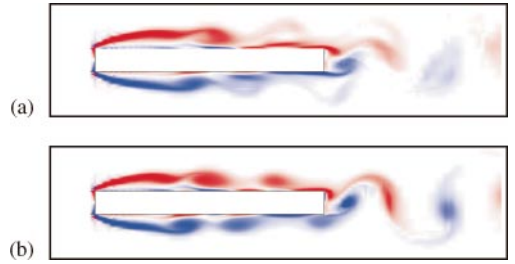


Figure 11. Vorticity plots of flow past a rectangular plate with $c/t = 10$ and $Re = 350$. The top plot, (a), shows span-averaged vorticity from a three-dimensional simulation. The bottom plot, (b), shows the corresponding vorticity field from a two-dimensional simulation. Opposite-signed vorticity is coloured red and blue.

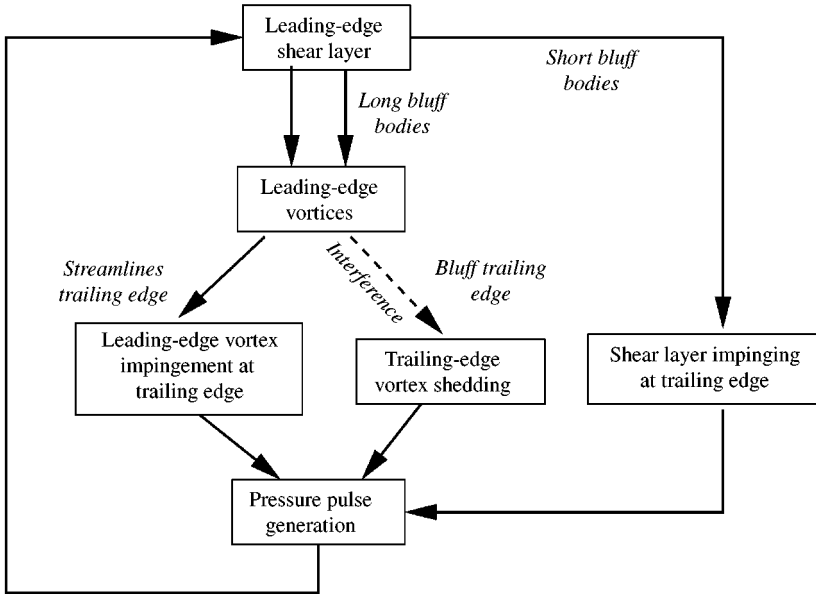


Figure 8. Schematic of feedback loops of locked vortex shedding for blunt leading-edge plates with either blunt or streamlined trailing edges.

of the technique used here enforced periodic boundary conditions on the spanwise boundaries. This allowed only discrete spanwise wavelengths (which is more restrictive for instabilities of longer wavelengths) to be captured.

3.3.1. Elliptical leading-edge plates

Simulations were performed for the flow around elliptical leading-edge plates with a 5 : 1 axes ratio and ratios of $c/t = 7.5$ and 2.5 . Two spanwise wake shedding modes were observed similar to Modes A and B for a circular cylinder (Williamson 1988). The spanwise wavelengths in the current simulations were generally larger for these plates possibly due to the thicker boundary layers near the trailing edge and the resulting vortices being more diffused.

Simulations with $c/t = 2.5$ have captured the two shedding modes in the transition process. The simulation captured a long wavelength flow structure at $Re = 300$ with topology consistent with Mode A shedding (see Figure 9). As only one wavelength of this flow structure was captured within the domain ($2\pi t$), there is some uncertainty as to which is the most unstable wavelength. There are smaller wavelengths that develop in certain shedding cycles. This could be either a competition between shedding modes or a result of the restrictive domain. At $Re = 350$, Mode A shedding is suppressed and the presence of some (streamwise vortical) flow structures consistent with Mode B shedding is apparent. The wavelength of these structures is uncertain because they are sporadic and not uniform across the span. When the Reynolds number is increased to $Re = 380$, these structures become more intense and more regular (also see Figure 9). These flow structures have a spanwise wavelength of approximately $0.8t$. The simulations were able to capture three-dimensional vortical structures with topology similar to Mode A at $Re = 500$ and $c/t = 7.5$.

3.3.2. Rectangular plates

The flows around rectangular plates with $c/t = 6, 10$ and 13 were simulated at $Re = 350$ and 400 . No boundary layer spanwise instability was observed in the simulations with $c/t = 6$. Flow structures similar to those classified as Pattern B by Sasaki & Kiya (1991) were observed when $c/t = 10$ and 13 at both $Re = 350$ (see Figure 10) and 400 . These were hairpin-like structures arranged in a staggered manner on both sides of the plate. In all cases, two wavelengths were captured in the domain and therefore the spanwise wavelength was approximately $3t$. (Again, because of the discrete Fourier mode description, there is some uncertainty in this estimate.) The streamwise wavelengths were approximately $3t$ when $c/t = 10$ and $4t$ when $c/t = 13$. Both the streamwise and spanwise wavelengths are within the range of experimental uncertainty of those observed experimentally (Sasaki & Kiya 1991). Pattern A shedding (vortices aligned) has been more difficult to capture, possibly due to the shorter plate lengths employed in the simulations.

3.3.3. Comparison with two-dimensional simulations

In this section, several flow characteristics of the two- and three-dimensional simulations are compared. A motivation for this is to demonstrate that the two-dimensional simulations are semi-quantitatively correct even when the flow has undergone transition. The case considered here is the flow past a rectangular plate with $c/t = 10$ and $Re = 350$. The computational domain and resolution on a two-dimensional plane was identical in both cases. The Strouhal numbers, St , in the two- and three-dimensional cases were $St = 0.170$ and 0.174 , respectively. Figure 11 shows a comparison of the two-dimensional flow structures between the two- and three-dimensional simulations. The three-dimensional simulation is reduced to a two-dimensional plane by averaging across the span. The vorticity plots clearly show that both cases are locked to the third, $n = 3$, shedding mode. The main difference between the plots is the more diffuse leading-edge vortices in the three-dimensional case. Importantly, from the point of view of the controlling mechanism, as for the two-dimensional simulation, strong base shedding is also observed with trailing-edge vortices seen to form from the redeveloped boundary layer between the passing of leading-edge vortices.

4. CONCLUSIONS

A series of simulations of flows around blunt plates have been undertaken to test the hypothesis that the trailing-edge shedding plays an important role in the self-sustained oscillations observed in flows around rectangular plates. First, the flow around plates of different chord-to-thickness ratios, with elliptical leading and square trailing edges, was studied. No leading-edge vortex shedding was present and strong periodic trailing-edge shedding was found with frequency in line with previous observations. Next, the flow around rectangular plates of various chord-to-thickness ratios was investigated. Self-sustained oscillations were found to occur which, for most chord-to-thickness ratios, were strictly periodic. Distinct vortex shedding from both the leading and trailing edges was observed. It is concluded that the preferred frequency of oscillation (i.e., both leading- and trailing-edge shedding) is that of the trailing-edge shedding. However, the leading-edge vortices punctuate the redeveloped boundary layer on the plate surface from which the trailing-edge vortices form. As the plate chord-to-thickness ratio is increased, this results in a gradual decrease in the possible trailing-edge shedding frequency until the preferred frequency is again possible; at this stage, the frequency undergoes a step change. The three-dimensional simulations show three-dimensional structures forming both along the

plate surface and in the wake. The spanwise-averaged flow, however, shows a distribution of structures similar to the two-dimensional flow, including strong trailing-edge vortex shedding. Pattern B vortical structures along the plate, and Modes A and B structures in the wake, each similar to those observed previously experimentally, have been captured by the simulations.

In some other flows where there is an absence of trailing-edge vortex shedding, the mechanism leading to self-sustained oscillations may in fact be the feedback loop generated by the impinging shear layer or the impinging leading-edge vortices. Although neglected in previous studies of flows around rectangular plates, it would appear that the trailing-edge shedding is a powerful influence on the self-sustained oscillations observed at lower Reynolds numbers. It is concluded in these cases that the global instability is a combination of the impinging shear layer instability (ILEV) and the trailing-edge vortex shedding instability (TEVS).

ACKNOWLEDGEMENTS

The Australian Research Council is thanked for supporting these studies through Small and Large Grants. Mr Tan Boon Thong acknowledges the support of a Monash Graduate Scholarship and an International Postgraduate Research Scholarship.

REFERENCES

- BARKLEY, D. & HENDERSON, R. D. 1996 Three-dimensional Floquet stability analysis of the wake of a circular cylinder. *Journal of Fluid Mechanics* **322**, 215–241.
- CHERRY, N. J., HILLIER, R. & LATOUR, M. E. M. P. 1984 Unsteady measurements in a separated and reattaching flow. *Journal of Fluid Mechanics* **144**, 13–46.
- EISENLOHR, H. & ECKELMANN, H. 1988 Observations in the laminar wake of a thin flat plate with a blunt trailing edge. In *Proceedings of the Conference on Experimental Heat Transfer, Fluid Mechanics and Thermodynamics* (eds R. K. Shah, E. N. Ganic & K. T. Yang), pp. 264–268, 4–9 September, Dubrovnik, Yugoslavia.
- HOIRIGAN, K., MILLS, R., THOMPSON, M. C., SHERIDAN, J., DILIN, P. & WELSH, M. C. 1993 Base pressure coefficients for flows around rectangular plates. *Journal of Wind Engineering and Industrial Aerodynamics* **49**, 311–318.
- KARNIADAKIS, G. E., ISRAELI, M. & ORSZAG, S. A. 1991 High-order splitting methods for the incompressible Navier–Stokes equations. *Journal of Computational Physics* **97**, 414–443.
- KARNIADAKIS, G. E. & TRIANTAFYLLOU, G. S. 1992 Three-dimensional dynamics and transition to turbulence in the wake of bluff objects. *Journal of Fluid Mechanics* **238**, 1–30.
- MILLS, R., SHERIDAN, J., HOIRIGAN, K. & WELSH, M. C. 1995 The mechanism controlling vortex shedding from rectangular bluff bodies. In *Proceedings of the 12th Australasian Fluid Mechanics Conference* (ed. R. W. Bilger), pp. 227–230, 10–15 December, Sydney, Australia.
- MILLS, R. H. 1998 Vortex interaction in flows over bluff bodies. Ph.D. Dissertation, Department of Mechanical Engineering, Monash University, Melbourne, Australia.
- NAKAMURA, Y. 1996 Vortex shedding from bluff bodies with splitter plates. *Journal of Fluids and Structures* **10**, 147–158.
- NAKAMURA, Y., OHYA, Y. & TSURUTA, H. 1991 Experiments on vortex shedding from flat plates with square leading and trailing edges. *Journal of Fluid Mechanics* **222**, 437–447.
- NAKAMURA, Y. & NAKASHIMA, M. 1986 Vortex excitation of prisms with elongated rectangular, H and \vdash cross-sections. *Journal of Fluid Mechanics* **163**, 149–169.
- NAUDASCHER, E. & ROCKWELL, D. 1994 *Flow-Induced Vibrations: An Engineering Guide*. Rotterdam: A. A. Balkema.
- NAUDASCHER, E. & WANG, Y. 1993 Flow-induced vibration of prismatic bodies and grids of prisms. *Journal of Fluids and Structures* **7**, 341–373.
- OHYA, Y., NAKAMURA, Y., OZONO, S., TSURUTA, H. & NAKAYAMA, R. 1992 A numerical study of vortex shedding from flat plates with square leading and trailing edges. *Journal of Fluid Mechanics* **236**, 445–460.

- OZONO, S., OHYA, Y., NAKAMURA, Y. & NAKAYAMA, R. 1992 Stepwise increase in the Strouhal number for flows around flat plates. *International Journal of Numerical Methods in Fluids* **15**, 1025–1036.
- ROCKWELL, D. 1990 Active control of globally-unstable separated flows. In *Proceedings of the ASME Symposium on Unsteady Flows*, 3–9 June, Toronto, Canada.
- ROCKWELL, D. & NAUDASCHER, E. 1979 Self-sustained oscillations of impinging free shear layers. *Annual Review of Fluid Mechanics* **11**, 67–94.
- SASAKI, K. & KIYA, M. 1991 Three-dimensional vortex structure in a leading-edge separation bubble at moderate Reynolds numbers. *ASME Journal of Fluids Engineering* **113**, 405–410.
- SORIA, J., SHERIDAN, J. & WU, J. 1993 Spatial evolution of the separated shear layer from a square leading-edge plate. *Journal of Wind Engineering and Industrial Aerodynamics* **49**, 237–246.
- TAN, B. T., THOMPSON, M. C. & HOURIGAN, K. 1998 Flow around long rectangular plates under cross-flow perturbations. *International Journal of Fluid Dynamics* (<http://elecpress.monash.edu.au/IJFD>) **2**, Article 1.
- THOMPSON, M. C., HOURIGAN, K. & SHERIDAN, J. 1994 Three-dimensional instabilities in the wake of a circular cylinder. In *Proceedings of the International Colloquium on Jets, Wakes and Shear Layers*, 18–20 April, Melbourne, Australia.
- THOMPSON, M. C., HOURIGAN, K. & SHERIDAN, J. 1996 Three-dimensional instabilities in the wake of a circular cylinder. *Experimental and Thermal Fluid Science* **12**, 190–196.
- WILLIAMSON, C. H. K. 1988 The existence of two stages in the transition to three-dimensionality of a cylinder wake. *Physics of Fluids* **31**, 3165–3168.